The HKU Scholars Hub   The University of Hong Kong   香港大學學術庫

Title	Mixed integral-differential skin-effect models for PEEC electromagnetic solver
Author(s)	Antonini, G; Ruehli, A; Jiang, L
Citation	The IEEE 20th Conference on Electrical Performance of Electronic Packaging and Systems (EPEPS 2011), San Jose, CA., 23-26 October 2011. In Proceedings of IEEE 20th EPEPS, 2011, p. 177-180
Issued Date	2011
URL	http://hdl.handle.net/10722/158767
Rights	IEEE Topical Meeting on Electrical Performance of Electronic Packaging Proceedings. Copyright © IEEE.

Mixed Integral-Differential Skin-effect Models for PEEC Electromagnetic Solver

Giulio Antonini
Dipartimento di Ingegneria Elettrica
e dell'Informazione
Università degli Studi dell'Aquila
I-67040 Monteluco di Roio, L'Aquila, Italy
Email: giulio.antonini@univaq.it

Albert E. Ruehli
UMR/MST EMC Laboratory
Missouri University
of Science and Technology
Rolla, MO 65409, USA
Email: albert.ruehli@gmail.com

Lijun Jiang
The University of Hong Kong
Dept. of Electrical
and Electronic Engineering
Hong Kong
Email: jianglj@hku.hk

Abstract—**Efficient modeling of the broadband skin-effect for conducting 3D shapes is a challenging issue for the solution of large electromagnetic problems. The inclusion of such models in an EM solver can be very costly in compute time and memory requirements. Several properties of a model are desirable for the solution of practical problems such as the broadband frequency domain or the time domain applicability. In this paper, we present a model which meets some of these challenges and which is suitable for the PEEC solution method.**

I. INTRODUCTION

The Partial Element Equivalent Circuit (PEEC) technique for 3D electromagnetic models in the circuit domain has evolved over the years. Much progress has been made in the capabilities of electromagnetic PEEC modeling from its origin [1] to numerous extensions, including volume and surface-based techniques and non-orthogonal models [2]. It is a natural approach for the solution of combined circuits and electromagnetic problems in the circuit domain.

A challenging issue for the solution of large electromagnetic problems is the efficient modeling of the skin-effect for conducting planes and 3D shapes as they occur in interconnects and other similar geometries. Unfortunately, such models can be very costly, especially if an accurate solution is required. Of course, the key application of such models is in electromagnetic solvers.

Many skin-effect models exist for ElectroMagnetic (EM) codes for 2D-Transmission Lines (TL) [3], [4], [5], [6]. Such models are much easier to construct for several reasons. The TEM mode allows the decoupling of the inductance and capacitance solutions which are computed based on 2D solvers.

In this paper, we consider the Partial Element Equivalent Circuit (PEEC) solver. A skin-effect model, to be effective, needs to be applicable to non-orthogonal 3D geometries, it must be wide-band, covering several frequency decades and, possibly, the same model needs to be applicable for time and frequency domain. The last item based on experience is that having a solver which works both in the time and frequency domain has many advantages. A PEEC solver can be very similar to a SPICE circuit solver in that it works in both domains.

The majority of the conventional skin-effect models were not applicable for wide-band 3D problems. However, several researchers have recently made advances in skin-effect models for 2D and 3D problems. Among the integral equation based solutions is the 3D Volume Filament Model (VFI) as it was implemented [1], [7] and for non-orthogonal shapes in [2]. It seems to be one of the oldest 3D models other than the finite element solutions. In the 3D-VFI model, the conductors are subdivided into *filament cells* in all three directions. The model is very accurate but it can also be computationally expensive.

The aim of this work is to develop a 3D mixed integral-differential skin-effect model for a surface PEEC solvers similar to the 2D GSI model [8]. The interior part of the conductor is modeled as an RL circuit which is proved to exactly represent Maxwell's equations in the limit that displacement currents are neglected. Such a differential model is adopted to compute the surface impedance which is coupled to the exterior problem described by the surface electric field integral equation. For the case when the conductors are very thin, a simpler more conventional skin-effect model has been derived in [9] which is related to [10], [11].

II. DERIVATION OF CONDUCTOR IMPEDANCE MODEL

The total electric field inside of a conductor is given by

$$E(r,t) = \frac{J(r,t)}{\sigma} = -\frac{\partial A(r,t)}{\partial t} - \nabla \Phi(r,t) \qquad (1)$$

where
- $J(r,t)$ is the current density in the conductors;
- $A(r,t), \Phi(r,t)$ are the vector and scalar potentials respectively;
- σ is the electrical conductivity.

Equation (1) can be rewritten by expressing the irrotational (Coulombian) part of the electric field in terms of the rotational part and the total electric field:

$$
\begin{aligned}
E^c(r,t) &= -\nabla \Phi(r,t) = \frac{J(r,t)}{\sigma} + \frac{\partial A(r,t)}{\partial t} \\
&= E(r,t) + E^r(r,t) \qquad (2)
\end{aligned}
$$

$E = J/\sigma$ is the total electric field inside the conductor. Equation (2), in the x, y, z components, reads:

$$
\begin{aligned}
E_x^c &= E_x + E_x^r & (3a) \\
E_y^c &= E_y + E_y^r & (3b) \\
E_z^c &= E_z + E_z^r & (3c)
\end{aligned}
$$

Hence, the first curl-Maxwell's equation reads

$$\nabla \times \boldsymbol{E} = \nabla \times \boldsymbol{E}^r = -\frac{\partial \boldsymbol{B}}{\partial t} \tag{4}$$

$$\frac{\partial E_z^r}{\partial y} - \frac{\partial E_y^r}{\partial z} = -\mu \frac{\partial H_x}{\partial t} \tag{5a}$$

$$\frac{\partial E_x^r}{\partial z} - \frac{\partial E_z^r}{\partial x} = -\mu \frac{\partial H_y}{\partial t} \tag{5b}$$

$$\frac{\partial E_y^r}{\partial x} - \frac{\partial E_x^r}{\partial y} = -\mu \frac{\partial H_z}{\partial t} \tag{5c}$$

$$\Delta y \Delta z \left(\frac{\partial E_z^r}{\partial y} - \frac{\partial E_y^r}{\partial z} \right) = -\mu \frac{\Delta y \Delta z}{\Delta x} \frac{dI_x}{dt} \tag{6a}$$

$$\Delta x \Delta z \left(\frac{\partial E_x^r}{\partial z} - \frac{\partial E_z^r}{\partial x} \right) = -\mu \frac{\Delta x \Delta z}{\Delta y} \frac{dI_y}{dt} \tag{6b}$$

$$\Delta x \Delta y \left(\frac{\partial E_y^r}{\partial x} - \frac{\partial E_x^r}{\partial y} \right) = -\mu \frac{\Delta x \Delta y}{\Delta z} \frac{dI_z}{dt} \tag{6c}$$

which can be re-written as

$$\Delta V_y^r - \Delta V_z^r = L_x \frac{dI_x}{dt} \tag{7a}$$

$$\Delta V_z^r - \Delta V_x^r = L_y \frac{dI_y}{dt} \tag{7b}$$

$$\Delta V_x^r - \Delta V_y^r = L_z \frac{dI_z}{dt} \tag{7c}$$

where the rotational voltages are

$$V_x^r = E_x^r \Delta x, \quad V_y^r = E_y^r \Delta y, \quad V_z^r = E_z^r \Delta z \tag{8}$$

the currents are defined as

$$I_x = H_x \Delta x, \quad I_y = H_y \Delta y, \quad I_z = H_z \Delta z \tag{9}$$

and the inductances as

$$L_x = \mu \frac{\Delta y \Delta z}{\Delta x}, L_y = \mu \frac{\Delta x \Delta z}{\Delta y}, L_z = \mu \frac{\Delta x \Delta y}{\Delta z} \tag{10}$$

Equation (7) clearly shows the rotational nature of the induced electric field.

The second curl-Maxwell's equation, if the displacement current is neglected, reads

$$\frac{\partial H_z}{\partial y} - \frac{\partial H_y}{\partial z} = J_x \tag{11a}$$

$$\frac{\partial H_x}{\partial z} - \frac{\partial H_z}{\partial x} = J_y \tag{11b}$$

$$\frac{\partial H_y}{\partial x} - \frac{\partial H_x}{\partial y} = J_z \tag{11c}$$

Multiplying both sides of (11) by the cross section orthogonal to $k = x, y, z$, respectively, yields

$$\Delta y \Delta z \left(\frac{\partial H_z}{\partial y} - \frac{\partial H_y}{\partial z} \right) = \Delta y \Delta z J_x = I_x \tag{12a}$$

$$\Delta x \Delta z \left(\frac{\partial H_x}{\partial z} - \frac{\partial H_z}{\partial x} \right) = \Delta x \Delta z J_y = I_y \tag{12b}$$

$$\Delta x \Delta y \left(\frac{\partial H_y}{\partial x} - \frac{\partial H_x}{\partial y} \right) = \Delta x \Delta y J_z = I_z \tag{12c}$$
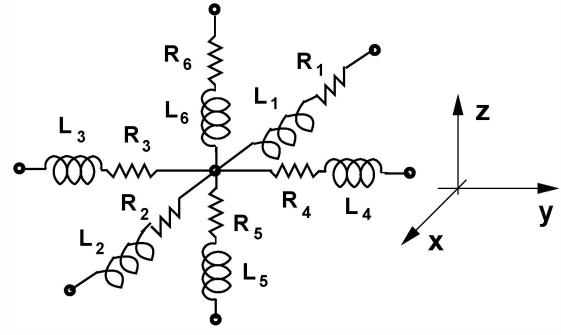

Fig. 1. 3D GSI conductor internal 3D skin-effect circuit.

which can be rewritten as

$$\Delta I_z - \Delta I_y = \Delta y \Delta z J_x = \frac{\Delta y \Delta z}{\Delta x} \sigma V_x \tag{13a}$$

$$\Delta I_z - \Delta I_x = \Delta x \Delta z J_y = \frac{\Delta x \Delta z}{\Delta y} \sigma V_y \tag{13b}$$

$$\Delta I_y - \Delta I_x = \Delta x \Delta y J_z = \frac{\Delta y \Delta z}{\Delta z} \sigma V_z \tag{13c}$$

where the total voltages are defined as

$$V_x = E_x \Delta x, \quad V_y = E_y \Delta y, \quad V_z = E_z \Delta z \tag{14}$$

Finally, equation (13) can be rewritten as

$$\Delta I_z - \Delta I_y = I_x = \frac{V_x}{R_x} \tag{15a}$$

$$\Delta I_z - \Delta I_x = I_y = \frac{V_y}{R_y} \tag{15b}$$

$$\Delta I_y - \Delta I_x = I_z = \frac{V_z}{R_z} \tag{15c}$$

where

$$R_x = \frac{\Delta x}{\sigma \Delta y \Delta z}, \quad R_y = \frac{\Delta y}{\sigma \Delta x \Delta z}, \quad R_z = \frac{\Delta z}{\sigma \Delta x \Delta y} \tag{16}$$

Integrating (3) along x, y and z directions yields:

$$V_x^c = V_x + V_x^r = R_x I_x + L_x \frac{dI_x}{dt} \tag{17a}$$

$$V_y^c = V_y + V_y^r = R_y I_y + L_y \frac{dI_y}{dt} \tag{17b}$$

$$V_z^c = V_z + V_z^r = R_z I_z + L_z \frac{dI_z}{dt} \tag{17c}$$

From (17), it can be seen that the EM field inside the conductor can be represented in a discrete form as an equivalent RL circuit on a structured mesh. The internal GSI conductor model corresponding to the above equation is given in Fig. 1.

Essentially, the conductors internal mesh as well as the circuit topology are the same as for the VFI model. The key difference is the inductance model. In the VFI model, all inductances are coupled. However, in this GSI model, only not coupled *differential* inductances are involved inside the conductor.

The mesh must be made nonuniform in order to capture the skin-effect while saving memory resources. A connectivity matrix $\boldsymbol{A}$ is used to relate branches and nodes of the mesh.

178

Any node can be assumed as reference without the capacitance model.

The enforcement of Kirchoff current law to each node and Ohm's law to each RL branch yields:

$$A I(t) = -I_{sg}(t) \qquad (18a)$$

$$A^T V(t) + L \frac{dI(t)}{dt} + R I(t) = 0 \qquad (18b)$$

In the complex frequency-domain, equations (18) read

$$A I(s) = -I_{sg}(s) \qquad (19a)$$

$$A^T V(s) + Z(s) I(s) = 0 \qquad (19b)$$

where $Z(s) = R + sL$.

III. Conductor surface impedance evaluation

Since only the surface cells are excited by the current sources, these latter can be expressed in terms of a surface connectivity matrix A_s as

$$I_{sg}(s) = A_s I_g(s) \qquad (20)$$

where $I_g(s)$ is an arbitrary vector of current sources.

Figure 2 shows the excitation of the equivalent RL network (cross-section view). Some algebraic manipulations allows the
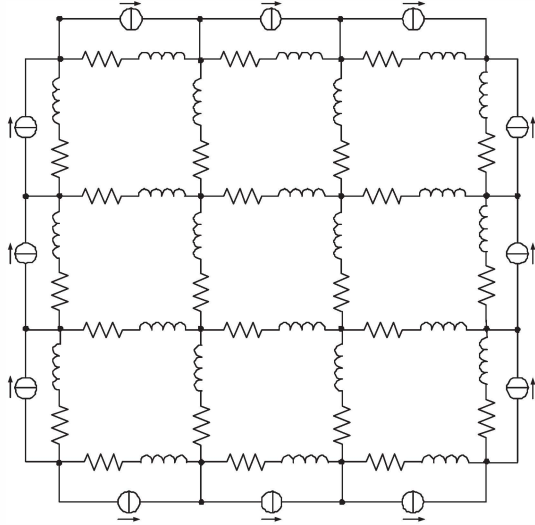

Fig. 2.   Schematic surface impedance cross-section circuit with surface current sources and four internal nodes and twelve external nodes.

node potentials to be related to the surface current sources as

$$V(s) = -\left(A Z^{-1}(s) A^T \right)^{-1} A_s I_{sg}(s)$$
$$= -Y^{-1}(s) A_s I_g(s) \qquad (21)$$

Finally, the voltage drop across and the current through each surface cell are

$$V_{sb}(s) = -A_s^T V(s) = A_s^T Y^{-1}(s) A_s I_g(s) \quad (22a)$$

$$I_{sb}(s) = Z_s^{-1}(s) V_{sb}(s) \qquad (22b)$$

	x_ℓ	y_ℓ	d	w	w_c
HShoe	35	50	6	10	0.4

where $Z_s(s)$ is the impedance matrix of the surface cells. The voltage drop across the resistance of surface cells is:

$$V_{sbr}(s) = R_s I_{sb}(s) = R_s Z_s^{-1} A_s^T Y^{-1}(s) A_s I_g(s) \qquad (23)$$

Hence, the surface impedance matrix is identified as

$$Z_{surf}(s) = R_s Z_s^{-1}(s) A_s^T Y^{-1}(s) A_s \qquad (24)$$

IV. PEEC solution for entire circuit

The external PEEC part of the model will not be described here since it is well known [2]. The resultant pcEFIE (potential-charge) integral equation model is best be described by the MNA equations in terms of the node potentials $\Phi(s)$ and the surface currents $I_s(s)$

$$\begin{bmatrix} sP^{-1} & -A_s \\ -A_s^T & -(Z_{surf}(s) + sLp_s) \end{bmatrix} \begin{bmatrix} \Phi(s) \\ I_s(s) \end{bmatrix} = \begin{bmatrix} I_g(s) \\ 0 \end{bmatrix} \qquad (25)$$

where Lp_s are the zero thickness surface partial inductance matrix, accounting for the magnetic field coupling occurring among surface currents, P is the coefficient of potential matrix describing the electric field coupling among surface charges, A_s is the connectivity matrix, $I_g(s)$ represents the vector of external current sources.

V. Numerical results

All the problems were run on a single-processor on a machine with 8 GB of RAM. The proposed methodology is tested by comparison with a standard 3D volume filament (VFI) based PEEC solver.

In a first test, we compute the input impedance of a single conducting block (dimensions $L = 10$ μm, $W = 5$ μm, $T = 3$ μm). Figure 3 shows the resistance and inductance as evaluated using the 3D proposed GSI method and the standard VFI approach.

The horseshoe geometry problem shown in Fig. 4 is considered and the dimensions are given in Table V. It consists of one layer with wide flat corners which leads to a current re-distribution with frequency. The input impedance is evaluated over a wide frequency range. The input resistance and inductance as computed by using the VFI approach and the proposed surface technique are shown in Fig. 5, exhibiting a reasonable agreement over the entire frequency range.

VI. Conclusions

In this work, a mixed integral-differential circuit 3D-GSI skin-effect model for a surface PEEC solver is presented. The strongly frequency dependent current distribution inside the conductor is captured by an equivalent RL circuit which is obtained providing a rigorous circuit interpretation for Maxwell's equations. We found it to be important to compare different techniques. The fact that we had access to different skin-effect solvers, such that we could validate the results, was essential for the success of our research.
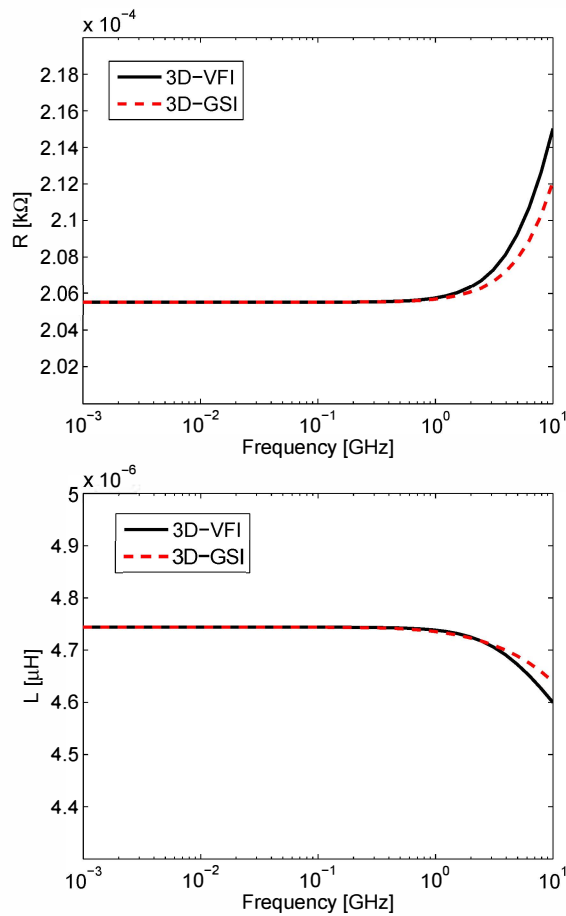
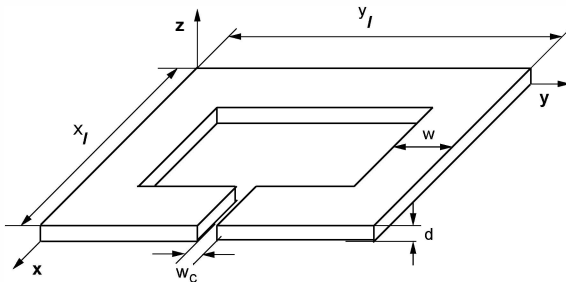Fig. 3.   Single block resistance (top) and inductance (bottom).

Fig. 5.   Horseshoe resistance (top) and inductance (bottom).

Fig. 4.   Horseshoe geometry.

References

[1] A. E. Ruehli, "Equivalent circuit models for three dimensional multiconductor systems," *IEEE Transactions on Microwave Theory and Techniques*, vol. MTT-22, no. 3, pp. 216–221, Mar. 1974.

[2] A. E. Ruehli, G. Antonini, J. Esch, J. Ekman, A. Mayo, and A. Orlandi, "Non-orthogonal PEEC formulation for time and frequency domain EM and circuit modeling," *IEEE Transactions on Electromagnetic Compatibility*, vol. 45, no. 2, pp. 167–176, May 2003.

[3] C. S. Yen, Z. Fazarinc, and R. Wheeler, "Time-domain skin-effect model for transient analysis of lossy transmission lines," *Proceedings of the IEEE*, vol. 70, pp. 750–757, Jul. 1982.

[4] T. R. Arabi, A. T. Murphy, T. K. Sarkar, R. F. Harrington, and A. R. Djordjevic, "On the modeling of conductor and substrate losses in multiconductor, multidielectric transmission line systems," *IEEE Transactions on Microwave Theory and Techniques*, vol. 39, no. 7, pp. 1090–1097, Jul. 1991.
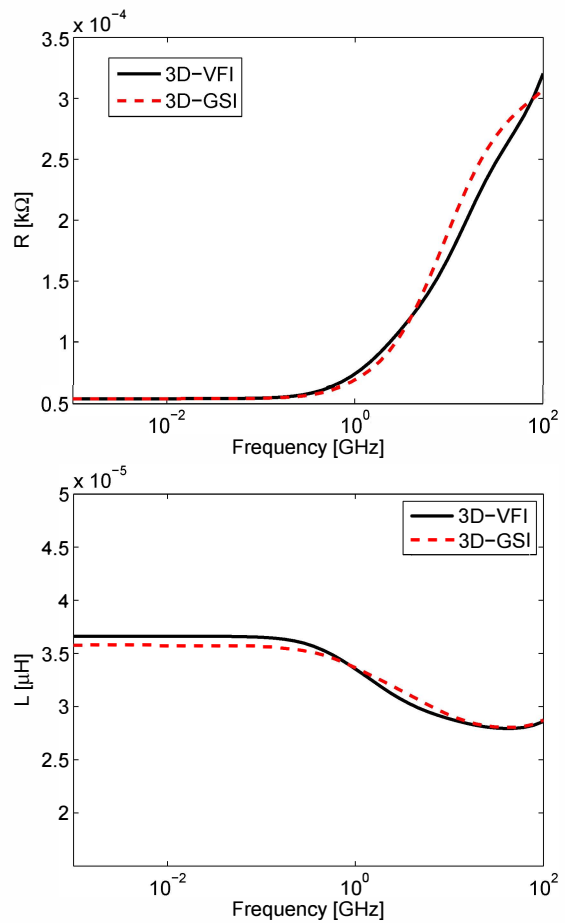
[5] M. J. Tsuk and J. A. Kong, "A hybrid method for the calculation of the resistance and inductance of transmission lines with arbitrary cross sections," *IEEE Transactions on Microwave Theory and Techniques*, vol. 39, no. 8, pp. 1338–1347, Aug. 1991.

[6] F. Bouzidi, H. Aubert, D. Bajon, and H. Baudrand, "Equivalent network representation of boundary conditions involving generalized trial quantities–application to lossy transmission lines with finite metallization thickness," *IEEE Transactions on Microwave Theory and Techniques*, vol. MTT-45, no. 6, pp. 869–876, Jun. 1997.

[7] M. Kamon, M. J. Tsuk, and J. White, "FastHenry: A multipole-accelerated 3-D inductance extraction program," in *Proc. of the Design Automation Conference*, Jun. 1993, pp. 678–683.

[8] K. Coperich, A. E. Ruehli, and A. C. Cangellaris, "Enhanced skin effect for partial-element equivalent circuit PEEC models," *IEEE Transactions on Microwave Theory and Techniques*, vol. 48, no. 9, pp. 1435–1442, Sep. 2000.

[9] G. Antonini and A. E. Ruehli, "Skin-effect model for time and frequency domain PEEC solver," in *Proc. of the IEEE Int. Symp. on Electromagnetic Compatibility*, Long Beach, CA, Aug. 2011.

[10] L. Daniel, A. Sangiovanni-Vincentelli, and J. White, "Proximity templates for modeling of skin and proximity effects on packages and high-frequency interconnect," in *Proc. Internat. Conference on Computer Aided Design*, Jun. 2002, pp. 326–333.

[11] M. Al-Qedra, J. Aronsson, and V. Okhamtovski, "A novel skin-effect based surface impedance formulation for broadband modeling of 3-d interconnects with electrical field integral equation," *IEEE Transactions on Microwave Theory and Techniques*, vol. 58, no. 12, Dec. 2010.